Biometals (2024) 37:971–982
https://doi.org/10.1007/s10534-024-00589-y

RESEARCH

Biogenic Ag_2O nanoparticles with "Hoja Santa" (*Piper auritum*) extract: characterization and biological capabilities

Dalia S. Aguilar-Ávila · M. Reyes-Becerril · Carlos A. Velázquez-Carriles · Gabriela Hinojosa-Ventura · María E. Macías-Rodríguez · Carlos Angulo · Jorge M. Silva-Jara

Received: 17 October 2023 / Accepted: 8 February 2024 / Published online: 26 February 2024

Abstract The 'sacred leaf' or "Hoja Santa" (*Piper auritum* Kunth) has a great value for Mexican culture and has gained popularity worldwide for its excellent properties from culinary to remedies. To contribute to its heritage, in this project we proposed the green synthesis of silver oxide nanoparticles (Ag_2O NPs) using an extract of "Hoja Santa" (*Piper auritum*) as a reducing and stabilizing agent. The synthesized Ag_2O NPs were characterized by UV–Visible spectroscopy (plasmon located at 405 nm), X-ray diffraction (XRD) (particle size diameter of 10 nm), scanning electron microscopy (SEM) (particle size diameter of 13.62 ± 4.61 nm), and Fourier-transform infrared spectroscopy (FTIR) (functional groups from "Hoja Santa" attached to nanoparticles). Antioxidant capacity was evaluated using DPPH, ABTS and FRAP methods. Furthermore, the antimicrobial activity of NPs against a panel of clinically relevant bacterial strains, including both Gram-positive (*Staphylococcus aureus*) and Gram-negative bacteria (*Salmonella* Enteritidis and *Escherichia coli* O157:H7), was over 90% at concentrations of 200 µg/mL. Additionally, we assessed the antibiofilm activity of the NPs against *Pseudomonas aeruginosa* (reaching 98% of biofilm destruction at 800 µg/mL), as biofilm formation plays a crucial role in bacterial resistance and chronic infections. Moreover, we investigated the impact of Ag_2O NPs on immune cell viability, respiratory burst, and phagocytic activity to understand their effects on the immune system.

Keywords Silver oxide nanoparticles · Green synthesis · *Piper auritum* · Antimicrobial activity · Antioxidant activity · Immune response

D. S. Aguilar-Ávila · G. Hinojosa-Ventura
Chemical Engineering Department, Universidad de Guadalajara, CUCEI, Blvd. Marcelino García Barragán 1421, Olímpica, 44430 Guadalajara, Jalisco, Mexico

M. Reyes-Becerril · C. Angulo
Immunology & Vaccinology Group, Centro de Investigaciones Biologicas del Noroeste (CIBNOR), Av. Instituto Politecnico Nacional 195, Playa Palo de Santa Rita Sur, 23096 La Paz, BCS, Mexico

C. A. Velázquez-Carriles · M. E. Macías-Rodríguez · J. M. Silva-Jara (✉)
Pharmacobiology Department, Universidad de Guadalajara, CUCEI, Blvd. Marcelino García Barragán 1421, Olímpica, 44430 Guadalajara, Jalisco, Mexico
e-mail: jorge.silva@academicos.udg.mx

C. A. Velázquez-Carriles
Biological, Synthetic and Materials Engineering Department, Universidad de Guadalajara, CUTlajomulco, Carretera Tlajomulco – Santa Fé km 3.5, 595, Lomas de Tejeda, 45641 Tlajomulco de Zúñiga, Jalisco, Mexico

Introduction

By 2050, global fatalities and the emergence of antimicrobial resistance will become a significant worldwide issue, posing a substantial threat to public health and healthcare systems. The misuse and overuse of

conventional antibiotics have resulted in the development of bacteria that are resistant to multiple drugs, rendering current treatments ineffective (Tang et al. 2023). As a consequence, there is an increasing emphasis on discovering alternative antimicrobial agents that are more potent and have fewer adverse effects. Also, within the food industry, the presence of biofilms is particularly alarming as it enhances the pathogenicity of foodborne bacteria. Generally, little to no attempt is made to eliminate these microorganisms from the processing environment. However, biofilms formed by pathogenic microorganisms and decomposing microorganisms serve as unfavorable reservoirs for microbial growth. Hence, it is crucial to identify effective strategies to combat biofilm formation (Liu et al. 2023).

"Hoja Santa", also known as the "sacred leaf," derives its name from the respect it has garnered among different indigenous and Mayan cultures due to its remarkable characteristics. Belonging to the *Piperaceae* family, which is closely related to the popular black pepper plant, this plant features sizable heart-shaped leaves that can grow up to a foot long (Fig. 1). These leaves emit a delightful aroma reminiscent of anise, mint, and black pepper, making them a highly desirable ingredient in both traditional and contemporary culinary practices (Salleh 2021).

"Hoja Santa", apart from its culinary allure, has been highly valued for its diverse medicinal properties. For generations, traditional healers have acknowledged its potential as a natural treatment for digestive problems, respiratory disorders, and skin ailments. The leaves are commonly infused into teas or applied externally in poultices to harness their healing properties. Furthermore, research has revealed that "Hoja Santa" exhibits antimicrobial, antioxidant, and hypoglycemic characteristics, underscoring its significance as a valuable botanical resource (Pérez-Gutiérrez 2016; Salleh 2021).

Fig. 1 The sacred leaf or "Hoja Santa"

One promising area of investigation involves utilizing nanomaterials as agents to combat microbial activity. Silver nanoparticles (AgNPs) have demonstrated broad spectrum antimicrobial effects against various harmful bacteria. However, the conventional synthesis of AgNPs often involves the use of harmful chemicals, which raises concerns about potential negative impacts on both human health and the environment (Jaswal and Gupta 2023). To address these concerns, researchers have explored environmentally friendly synthesis methods that utilize natural extracts or plant-based materials to produce nanoparticles. Utilizing plant extracts in nanoparticle synthesis offers several advantages, including environmental sustainability, cost-effectiveness, and the potential for enhanced antimicrobial properties (Dawadi et al. 2021). "Hoja Santa" (*Piper auritum*), a plant native to México, is renowned for its antimicrobial properties. It contains bioactive compounds such as essential oils, phenolics, and flavonoids, which have exhibited promising antimicrobial effects against a wide range of bacterial pathogens (Aguilar-Urquizo et al. 2020; Chacón et al. 2021).

The objective of this study was to investigate the environmentally friendly production and characterization of Ag_2O nanoparticles (Ag_2O NPs) using aerial parts of "Hoja Santa" extract through solid-state techniques. Additionally, the study aimed to evaluate the antimicrobial, antibiofilm, and immunomodulating properties of these nanoparticles. The results of this research have the potential to advance the development of innovative antimicrobial agents that are both effective against bacterial resistance and environmentally sustainable.

Materials and methods

Piper auritum aqueous extract

Piper auritum plant was obtained from local markets of Guadalajara, Mexico. Aerial parts were disinfected in a

2 mg/mL solution of NaClO by immersion for 10 min, subsequently, they were washed with distilled water, and allowed to dry in oven (L–C Oven, Mechanically Convected) at 40 °C. Dry plants were grounded and reserved at 4 °C until use. Then, a solution of 1:10 (m/V) was prepared with 100 mL of distilled water and brought to a boil, keeping the temperature at 100 °C for 5 min. After, the solution was filtered through Whatman N°1 filter paper, and aqueous extract was stored in amber flasks at − 20 °C until use (Silva-Jara et al. 2020).

Silver nanoparticle synthesis (Ag_2O nps)

Briefly, 50 mL of a $AgNO_3$ (3 mM) solution was prepared, then 15 mL of *P. auritum* extract were added and the solution was kept in constant agitation in the dark for 24 h at room temperature. Posteriorly, the solution was centrifuged at 6000 rpm at 25 °C for 30 min (Labo-Gene, LZ-1580R) and pellet was dried in the oven at 80 °C for 8 h.

Characterization

Surface plasmon resonance was measured in a UV–Vis spectrophotometer (NanoDrop 2000, Thermo Scientific) from an aliquot of synthesis solution. Fourier-transform infrared spectra (FT-IR) of *P. auritum* extract and Ag_2O NPs were collected in a range of 4000–400 cm^{-1} with 4 cm^{-1} resolution and 32 scans in a Cary 630 spectrophotometer (Agilent Technologies). X-ray diffractograms patterns were obtained in an X-ray Diffractometer (Malvern Panalytical Empyrean) from a 2θ angle of 5 to 70 with a step of 0.2 and collection time of 30 s. For morphology, scanning electron microscopy (SEM) was recorded in a FE-SEM (TESCAN, MIRA 3 LMU) with 15 kV of voltage.

Particle size analysis

DRX calculation

Debye-Scherrer equation through DRX parameters was calculated as follow:

$$D = \frac{0.9\lambda}{\beta \cos\theta},$$

where λ wavelength in DRX was 1.54059 nm, β is considered as 'full width at a half maximum' (FWHM), θ is the angle of diffraction, and D is the particle size in nm.

SEM image processing

The particle size distribution was calculated using ImageJ software v1.53 and the histogram was fitted with Lorentz function.

Total phenolic content

Total phenolic content was determined following the procedure described by Singleton et al. (1999), with some modifications. 100 µL of Ag_2O NPs were added to 500 µL of distilled water and 100 µL of Folin-Ciocalteu (1:10 v/v), and the mixture was incubated for 7 min at room temperature. Then, 1 mL of $CaCO_3$ (7% m/v) was added and the solution was kept for 90 min in dark. A standard curve of gallic acid (0–250 µg/mL) was used for comparison. Absorbance was measured in a UV–Vis spectrophotometer (Optizen, POP) at 750 nm, and results were expressed as mg GAE/g (mg of gallic acid equivalent per g).

Antioxidant activity

2,2-diphenil-1-picrylhydrazil (DPPH) radical scavenging was determined according to Brand-Williams et al. (1995) using ascorbic acid (AA) in the same concentrations as Ag_2O NPs for comparison and ethanol as control. Results were expressed as % inhibition determined with the equation:

$$\text{DPPH\%inhibition} = \frac{\text{Abs}_{\text{control}} - \text{Abs}_{\text{sample}}}{\text{Abs}_{\text{control}}} \times 100$$

For 2,2'-azino-bis(3-ethylbenzothiazoline-6-sulfonic acid) (ABTS), Li et al. (2008) procedure was followed with AA for comparison and ethanol as control. Results were expressed as mentioned for the DPPH measure. Ferric reducing antioxidant power (FRAP) was conducted with the methodology described by Benzie and Strain (1996) using a standard curve of AA. Results were calculated as mg EAA/mg (mg equivalent of ascorbic acid per mg).

Antimicrobial evaluation

Antibacterial activity of Ag_2O NPs was tested with microdilution and diffusion assays. Three bacterial strains (*Escherichia coli* ATCC 8739, *Salmonella* Enteritidis isolated from clinical cases, and *Staphylococcus aureus* ATCC 25923) were cultured in tryptic soy broth (TSB) for 24 h at 36 °C previously for tests. Then, concentration was adjusted to 1×10^6 cells/mL with optical density, OD600, in a spectrophotometer (OPTIZEN). For microdilution, 20 µL of each strain were added to a 96-well microplate with 20 µL of Ag_2O NPs solutions at 200, 500 and 800 µg/mL of concentration and 160 µL of TSB, using phosphate buffer solution (PBS) as negative control, while gentamicin 0.1% (m/v) was positive control (Castorena-Sánchez et al. 2023). Microplate was incubated for 24 h at 36 °C, then, optical density was measured in a microplate reader (BIORad) at 595 nm, and inhibition was determined with the equation:

$$\mathrm{BGIR}(\%) = \frac{\mathrm{Abs}_{\mathrm{control}} - \mathrm{Abs}_{\mathrm{sample}}}{\mathrm{Abs}_{\mathrm{control}}} \times 100,$$

where BGIR is the bacterial growth inhibition rate.

For diffusion test, bacterial strains were streaked in Müller-Hinton agar (MHA), holes were bored using a 1 mL sterile micropipette tip and 100 µL of Ag_2O NPs of each of the previous concentrations were added (200, 500 and 800 µg/mL). Plates were incubated as mentioned before and diameters of inhibition were measured. All experiments were performed in triplicate and the results were expressed as mean ± standard deviation.

Antibiofilm activity

Biofilm is a protective mechanism that some bacteria form in order to protect against lethal components or treatments. In order to study the capacity of Ag_2O NPs to inhibit biofilm formation, O'Toole (2011) methodology was followed, using *Pseudomonas aeruginosa* ATCC 83759. Briefly, *P. aeruginosa* strain was cultured in Luria-Bertani broth overnight at 36 °C, and then, a 1:10 dilution was made in fresh medium supplemented with arginine (0.04% w/v). In a 96-well microplate 100 µL of the strain were added with 20 µL of Ag_2O NPs in different concentrations. Microplate was incubated for 24 h at 36 °C, followed by 2 washes with distilled water by immersion; plate was allowed to dry. Next, 125 µL of crystal violet (0.1% m/v) (Romero-García et al. 2023) was added and incubated at 25 °C for 15 min, then, it was washed as mentioned before. Finally, 125 µL of acetic acid (30% v/v) were added and incubated for 15 min at room temperature, and then, they were transferred to a new plate and read at 595 nm in a microplate reader (BIOrad). Results were determined with the equation:

$$\%\text{biofilm inhibition} = \left(1 - \frac{(\mathrm{Abs}_{\mathrm{sample}} - \mathrm{Abs}_{\mathrm{blank})}}{(\mathrm{Abs}_{\mathrm{control}} - \mathrm{Abs}_{\mathrm{blank}})}\right) \times 100,$$

where ABS is the absorbance of sample (*P. aeruginosa* in contact with Ag_2O NPs), control (*P. aeruginosa* without treatment) and blank is acetic acid 30% (v/v) in distilled water.

Immunostimulant test

Broiler chicken bone marrow leukocytes extraction

The studies presented in this manuscript were approved by the Bioethical Committee of the Autonomy University of Baja California Sur following international and national regulations (NOM-062-ZOO-1999 and NOM-008-ZOO-1994). Five broiler chickens were sampled at week 4. Before sampling, the birds were starved for 24 h. The right tibia was dissected sterilely from the slaughtered birds and the soft tissues of bone marrow were removed, passed through 100 µm cell strainer (BD Falcon, Franklin Lakes, NJ, USA), and transferred to 10 mL of an sRPM (RPMI-1640, Gibco, Grand Island, NY, USA; culture medium containing P/S, 10% FCS). To recollect leukocytes following the methodology described by Angulo et al. (2017). Briefly, cell suspension was centrifuged (500 *g*, 45 min, 23 °C), and leucocyte layer was collected and washed with sRPMI medium (800 *g*, 10 min, 23 °C). Cells were observed and counted in a TC20 Coulter Particle Counter (BioRad, Hercules, CA, USA) and adjusted to 10^6 cells/mL of sRPMI.

Cell viability

Resazurin method was used to determine cell viability of leukocytes following the method reported by

Riss et al. (2016). Cells without any treatment and leukocytes incubated with DMSO were used as controls. Briefly, cells were dispensed in 96-well plates (90 µL 1×10^6 cells/mL) and incubated with 10 µL/well of Ag_2O NPs at each concentration previously used. Twenty-four hours later, cells were stained with 10 µL resazurin solution (Sigma, St. Louis, MO, USA) and incubated at 37 °C and 5% CO_2 for 4 h. Then, cells fluorescence was measured in Varioskan™ Flash Multimode Reader (Thermo Scientific, Waltham, MA, USA) with excitation at 530 nm and emission at 590 nm. The assay was performed in sixtyfold and viability (%) was calculated using the following formula:

$$\text{Viability}(\%) = \frac{\text{Abs}_{\text{sample}}}{\text{Abs}_{\text{negativecontrol}}} \times 100,$$

where $\text{Abs}_{\text{negative control}}$ is the absorbance of the cells without treatment.

Phagocytosis activity

Phagocytosis activity was evaluated according to the methodology described by Wang et al. (2017). After cultivation for 24 h, the nonadherent cells were removed with micropipette and the remaining ones were washed twice with PBS. Then, 100 µL of neutral red solution (0.33% in DPBS) were dispensed followed by an incubation for 4 h. Posteriorly, the neutral red solution was discarded, washing with PBS twice. A solution of ethanol and acetic acid (cell lysate/1:1 ratio) was added and incubated for 1 h, and the absorbance was recorded at 540 nm (iMark™ BioRad, Hercules, CA, USA).

Respiratory burst activity

Respiratory burst activity of the leukocytes isolated from bone marrow, with and without Ag_2O NPs at different concentrations, was measured with nitroblue tetrazolium (NBT) according to Kemenade et al. (1994). Leukocytes were incubated with NBT (1 mg/mL, Sigma, St. Louis, MO, USA), and after two hours of incubation, the reaction was stopped with 100 µL of methanol (70% v/v). The plates were air-dried, and 120 µL of 2 M potassium hydroxide and 140 µL DMSO were added to each well. The optical density (OD) was measured at 655 nm in a microplate reader (iMark™ BioRad, Hercules, CA, USA).

Statistical analysis

Data was analyzed using StatGraphics Centurion 19 (V19.5.01). ANOVA and Tukey tests were conducted, and results are expressed as mean ± standard deviation.

Results and discussion

Surface plasmon resonance

Figure 2 shows the UV–Vis spectrum with a peak at 405 nm, which is characteristic of the plasmon attributed to the confinement of the nanoparticles that have been previously documented and confirm that the synthesis of Ag_2O NPs was achieved. Characteristic color ranging from yellow to light brown after 24 h of synthesis was observed (Shehabeldine et al. 2021; Ali et al. 2022).

Fourier transform infrared spectroscopy

In Fig. 3, the IR spectrum can be observed, where the peak at 3338 cm^{-1} corresponds to the –OH

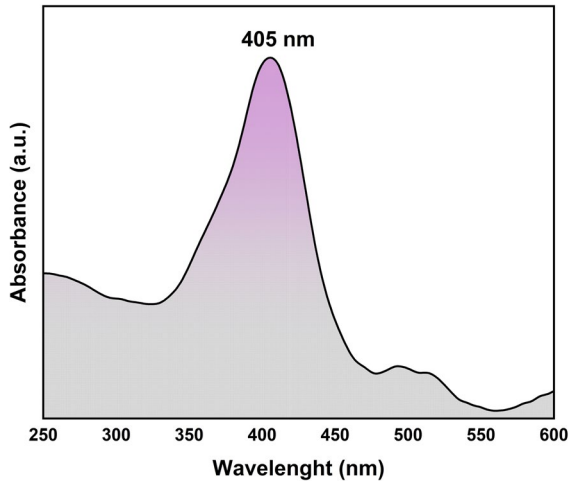

Fig. 2 Surface plasmon resonance of silver oxide nanoparticles synthesized using "Hoja Santa" leaf extract

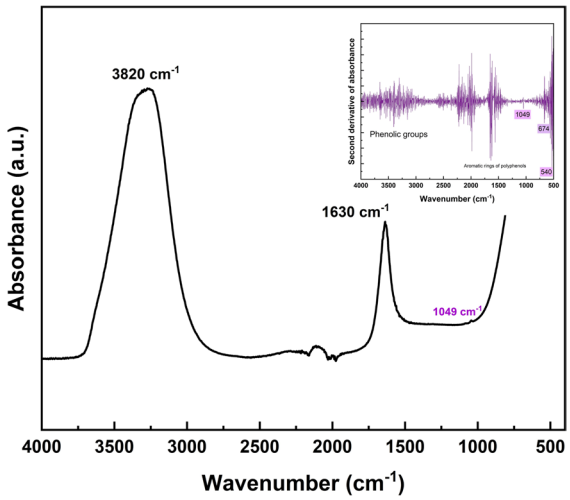

Fig. 3 Infrared spectrum of silver oxide nanoparticles (inset: second derivative of the infrared range)

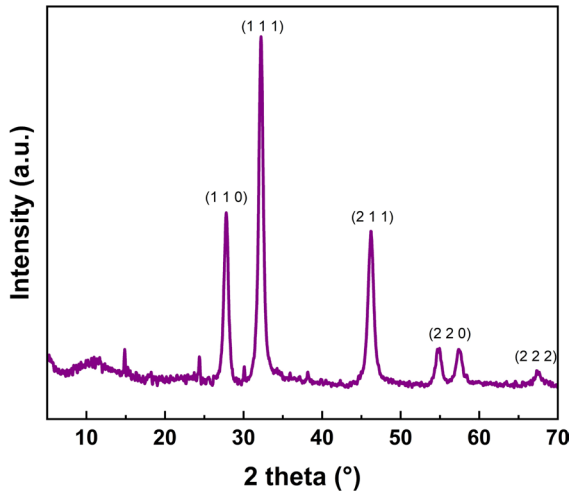

Fig. 4 Diffractogram of silver oxide nanoparticles

group, which has been previously referenced for phenolic compounds and flavonoids. The vibrations around 1640 cm^{-1} can be attributed to aromatic ring vibrations, likely associated with polyphenols in previous publications on biogenic nanoparticles synthesized with phytochemicals (Jabbar et al. 2020). To better appreciate the fingerprint region, a second derivative was performed on the original spectrum as a criterion for elucidating contributions that vibrate in these regions (inset in Fig. 3). Three signals are observed at 1049, 674, and 540 cm^{-1}; the signal at 1049 cm^{-1} can be attributed to the C–O vibration, the signal at 674 cm^{-1} corresponds to moieties of polyphenols (Manik et al. 2020), and finally, around 540 cm^{-1}, there is an essential vibration for metallic groups, which could refer to silver nanoparticles attached to hydroxyl groups from the extract (Al-Rajhi et al. 2022) or the formation of Ag–O interactions (Dharmaraj et al. 2021), thus corroborating that the synthesis was carried out.

X-ray diffraction (XRD)

Figure 4 shows the diffractogram for the silver nanoparticles, revealing the characteristic Bravais lattice or Miller indices for the silver oxide structure at angles 27.78°, 32.22°, 46.19°, 54.80°, and 67.37°, corresponding to the planes (1 1 0), (1 1 1), (2 1 1), (2 2 0), and (2 2 2), respectively. These correspond to a face-centered cubic structure and are consistent with previous studies on biogenic Ag_2O particles (Dhoondia and Chakraborty 2012; Dharmaraj et al. 2021) and the international database (JCPDS 76-1393) (Fowsiva and Madhumitha 2019). The results demonstrate the transition from Ag to Ag_2O formation, attributed to the amount of extract used (Banua and Han 2020). The crystal size was also calculated using the Debye–Scherrer equation, resulting in a length of 10 nm.

Scanning electron microscopy

Figure 5a shows the SEM micrograph of the Ag_2O nanoparticles with spherical structures, and it displays an approximate distribution (Fig. 5b) of 13.62 ± 4.61 nm according to the histogram, which is consistent with the approximate size obtained from X-ray diffraction.

Antioxidant activity

Ag_2O NPs total polyphenols, estimated with Folin-Cicoalteu, was of 9.25 ± 2.60 mg GAE/g. Percentage of inhibition of ABTS, DPPH and FRAP radicals is depicted in Fig. 6. ABTS inhibition (Fig. 6A) was $90.7 \pm 0.83\%$ for concentrations between 50 and 300 µg/mL of Ag_2O NPs. Interestingly, silver

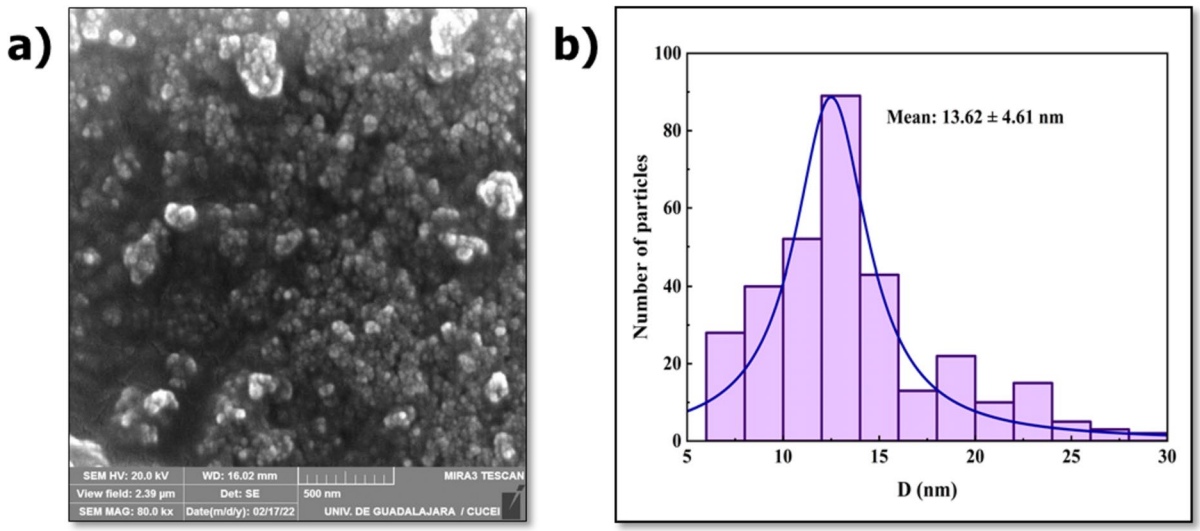

Fig. 5 The morphology and particle size of Ag_2O nanoparticles (NPs) are as follows: **a** SEM micrograph and **b** Size distribution histogram

nanoparticles inhibition was higher than ascorbic acid activity up to 150 µg/mL, a commercial antioxidant. In DPPH (Fig. 6B), inhibition was concentration-dependent from 50 to 250 µg/mL, exhibiting higher percentages than ascorbic acid. Similar behavior was found for FRAP test, with results ranging from 0.284 to 14.349 mg EAA / mg Ag_2O NP (Fig. 6C).

Previously, Essghaier et al. (2022) reported that silver nanoparticles obtained from green synthesis using *Scabiosa atropurpurea* extract had an IC50 value for DPPH radical of around 0.112 ± 0.210 mg/mL, a little lower than the one obtained here. DPPH assay is based on the color change of the solution when its H is donated to the antioxidant agent. Bhakya et al. (2022) found a similar concentration-dependent behavior for nanoparticles synthesis from *Helicteres isora* root extract; a 90% inhibition was determined, and it is suggested that not only silver produces this inhibition, but some residues of the extract used for the synthesis could be acting as well.

Antibacterial activity

Gram-negative bacterial strains *E. coli* and *S.* Enteritidis, and the Gram-positive bacterial strains *S. aureus*, were used to evaluate the antibacterial activity potential of Ag_2O NPs. Inhibition halo diameter (mm) of Ag_2O NPs was determined by using the diffusion method and results are shown in Table 1. The diameters of inhibition of *E. coli* and *S.* Enteritidis were 15.1–20.7 and 10.2–13.8 mm, respectively, while for *S. aureus*, it was 12.9–14.6 mm. According to the Duraffourd scale [Null (−) < 8 mm, Sensible (+) > 8 mm ≤ 14 mm, Very sensible (++) > 14 ≤ 20 mm; Highly sensible (+++) > 20 mm)] (Morillo-Carrillo and Balseca-Ibarra, 2018), *E. coli* was very sensible-highly sensible (++ for 200 and 500 µg/mL; +++ for 800 µg/mL) to Ag_2O NPs concentrations, while *S.* Enteritidis and *S. aureus* were sensible (+). The antibacterial activity of Ag2O NPs from *P. auritum* is consistent with previous research on AgNPs synthesized from other species of the same plant genus (Amaliyah et al. 2022; Dewi et al. 2023; Kanniah et al. 2021; Nguyen et al. 2021).

The bacterial growth inhibition rate (BGIR) was evaluated for the strains mentioned below at different concentrations of Ag_2O NPs. The results are shown in Fig. 7, where both Gram-negative and Gram-positive bacteria were inhibited at 99% in the three concentrations. The observed antibacterial activity of the Ag_2O NPs was higher against Gram-negative bacteria; those results could be due to the difference in molecular makeup of the cell walls (Corciova et al. 2019; Sneha et al. 2017). Ag_2O NPs obtained through green synthesis have been tested against other bacteria like *S.*

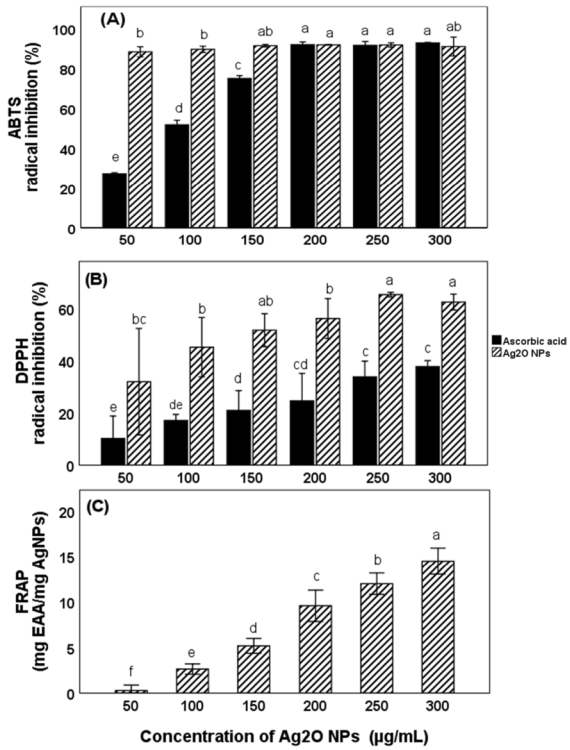

Fig. 6 Antioxidant effect of nanoparticles of silver oxide from *P. auritum.* **A** radical inhibition percent of different concentrations of Ag_2O NPs by ABTS assay, **B** radical inhibition percent of different concentrations of Ag_2O NPs by DPPH; **C** FRAP mg EAA/mg of Ag_2O NPs. Black bars correspond to ascorbic acid (control); the lines' bars are silver oxide nanoparticles. The figures show the mean with three measurements ($n=3$). Different letters indicate that there is a statistical difference between the treatments (Tukey, $p \leq 0.05$)

Table 1 Inhibition halo zone for silver oxide nanoparticles

Bacterial strain	Inhibition halo zone (mm)		
	200 µg/mL	500 µg/mL	800 µg/mL
Escherichia coli	15.1 ± 0.3^{a}	17.3 ± 0.3^{b}	20.7 ± 1.5^{c}
Salmonella Enteritidis	10.2 ± 0.2^{A}	11.7 ± 1.5^{AB}	13.8 ± 1.4^{B}
Staphylococcus aureus	12.9 ± 0.2^{I}	13.6 ± 0.5^{I}	14.6 ± 0.6^{II}

Different letters indicate that there is a statistically significant difference between concentrations (Tukey, p 0.05)

mutans and *L. acidophilus* (Manikandan et al. 2017), with bactericidal concentrations ranging in the same ones evaluated in this research.

The antibacterial mechanism of AgNPs has been described in several possible ways. The first one is by adhesion of AgNPs in the bacterial cell membrane, and the second one is by penetration of the AgNPs. In the first mechanism, silver nanoparticles are disturbed in their permeability and respiratory functions, and in the second way, AgNPs interfere with protein synthesis and destroy the DNA and RNA structures (Ibrahim et al. 2021; Awad et al. 2019; Ayromlou et al. 2019). Another aspect that can contribute to the antibacterial effect could be the presence of compounds with antimicrobial properties like phenols and flavonoids present in the extract of natural sources (Corciova et al. 2019).

Inhibition of biofilm formation

P. aeruginosa produces biofilm in growth-stress conditions. Three different concentrations of Ag_2O *NPs* were evaluated: 200, 500, and 800 µg/mL. Results in Fig. 8 show that the percentage inhibition of biofilm formation by *P. aeruginosa* exhibited a dose-dependent behavior; with the lower concentration the inhibition was of 80%, and for 500 and 800 µg/mL, it was around 90%, with no significant difference between the later ($p > 0.05$). Previous research studies about the antibiofilm activity of AgNPs against *P. aeruginosa* isolate showed that they inhibited biofilm growth depending on some factors such as concentration, source and especially size and surface area (de Lacerda Coriolano et al. 2021; Hetta et al. 2021). Mechanism of AgNPs include binding of the nanoparticle to the exopolysaccharide matrix of biofilm and cause ROS production, and finally, disruption of biofilm (de Lacerda Coriolano et al. 2021; Akar et al. 2023).

Inmunostimulant effect, phagocytosis activity and respiratory burst activity

Cell viability of broiler chicken leukocytes stimulated with silver nanoparticles is depicted in Fig. 9A. Viability was up to 91% at a concentration of 200 µg/mL of Ag_2O NPs, while at high concentration (800 µg/mL), this parameter dropped to 54%.

This also was observed in the cell viability test of normal lung cells upon different composite Ag2O/ZnS/GO/CA concentrations, observing a higher

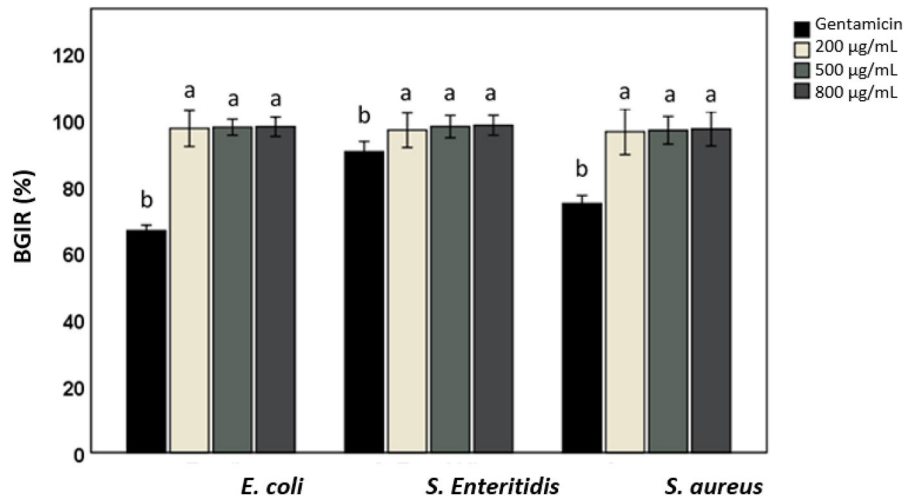

Fig. 7 Antibacterial properties of Ag_2O NPs from *P. auritum* on *E. coli, S. aureus*, and *S.* Enteritidis growth. The values of bars represent the mean and their standard. Different letters indicate that there is a statistically significant difference between the treatments (Tukey, p 0.05).

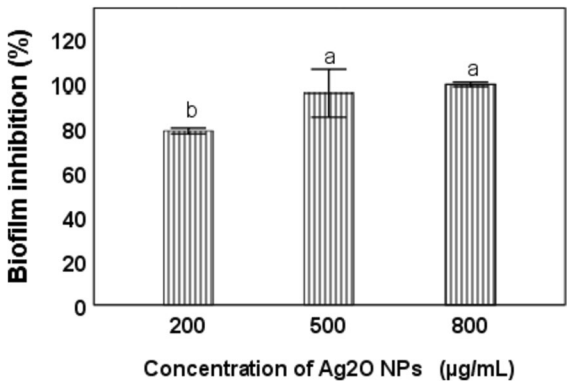

Fig. 8 Inhibition of biofilm formation of *P. aeruginosa* at different concentrations of Ag_2O NPs from *P. auritum*. The values of the bars represent the mean and their standard. Different letters indicate that there is a statistical difference between the treatments (Tukey, $p \leq 0.05$)

percentage of viability at low concentrations, around 1000 µg/mL (Alharthi et al. 2023).

Respiratory burst associated with reactive oxygen species functions as a mechanism to eliminate pathogens. In Fig. 9B, a dose dependent behavior regarding Ag_2O NPs concentration is observed. The presence of high oxidative compounds such as silver oxide favors the production of ROS, which acts as a method to eliminate these nanoparticles or possible threats (Paunovic et al. 2020). Also, the excess of ROS production may kill leukocytes, a strong relationship shown in the cell viability graph. In chickens supplemented with silver nanoparticles during growth, an increase in respiratory burst activity was observed compared to the control group (Ognik et al. 2016).

Phagocytosis activity of broiler chicken leukocytes is depicted in Fig. 9C. In low concentrations (200 µg/mL) higher activity was observed compared to the control group, although the difference was not significant ($p > 0.05$), while at higher nanoparticle concentrations (500 and 800 µg/mL), activity was significantly reduced. Phagocytosis is a process activated during inflammatory states as a method to eliminate pathogens that threaten the organism. It has been demonstrated that stimulation with silver nanoparticles during animal growth increases phagocytosis against pathogens such as *Staphylococcus aureus* 209P (Ognik et al. 2016), but nanoparticles can be accumulated in the lymphatic organs and thus, provoke an immunosuppression effect (Ahmadi 2012). These results correspond to the reduction of activity at higher concentrations of Ag_2O nanoparticles used in the present study.

Conclusion

Silver oxide nanoparticles were synthesized from *Piper auritum* ("Hoja Santa") aerial parts extracts. Characterization with X-ray Diffraction, Scanning Electron Microscopy and UV–Vis and FT-IR spectroscopy corroborated the crystal phase, morphology and particle size distribution.

Antioxidant, antimicrobial, antibiofilm formation, and cytotoxic activities were evaluated,

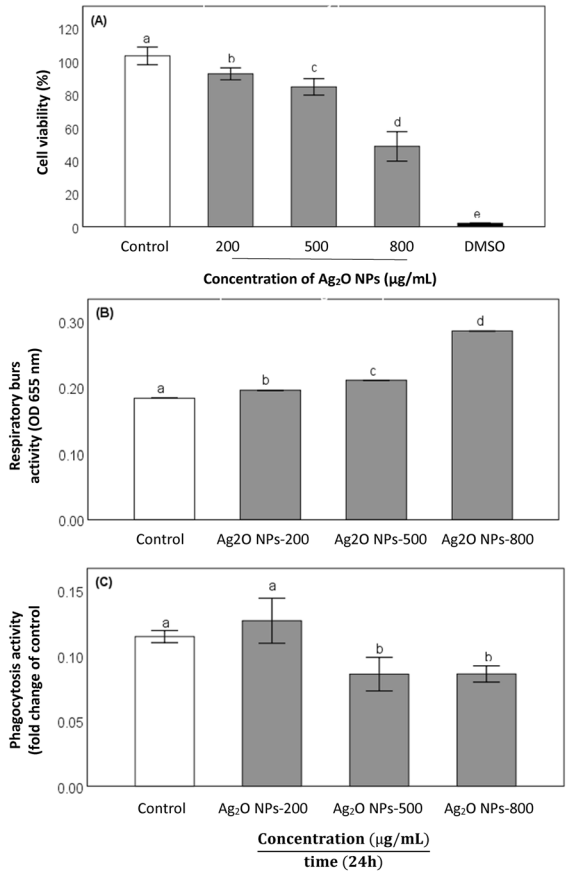

Fig. 9 **A** cell viability under different Ag_2O NPs from *P. auritum* amounts of leukocytes. Leukocytes untreated were utilized as a proliferation control, and DMSO functioned as a toxicity control. **B** Respiratory burst activity. **C** Phagocytosis activity. The mean and standard are illustrated by the values of the bars. A statistical difference between the treatments is indicated by a distinct letter. (Tukey, $p \leq 0.05$)

demonstrating superior antioxidant activity than compounds typically used in commercial products. As an antimicrobial agent, concentrations below 1 mg/mL exhibited inhibition above 90% for both Gram-positive and Gram-negative bacteria, and also, prevented biofilm formation of *Pseudomonas aeruginosa*.

Broiler chicken leukocytes had a viability of 90% at concentrations of 200 µg/mL, with high phagocytosis and respiratory burst activities enhanced. In this concentration, Ag_2O NPs can be used to eliminate pathogen threats and avoid compromising cell viability.

Results found in this research explores a green method to obtain silver oxide nanoparticles, and a possible way to apply them to chicken cultures.

Acknowledgements Thanks to Alma Mercado Gutiérrez for technical support and Sergio Oliva León for X-ray and SEM support.

Author contributions Aguilar-Avila: Writing and editing, data analysis. Reyes-Becerril: Immune experiments, writing and editing, resource provide, data analysis. Velázquez-Carriles: Experimental research, first draft writing, and editing, data analysis. Hinojosa-Ventura: Writing and editing, spelling checking, data analysis. Macías-Rodríguez: Resource provide, review. Angulo: Resource provide, review. Silva-Jara: First draft writing, experimental design, resource provide, writing editing, data analysis.

Funding Authors thank the Consejo Nacional de Humanidades, Ciencia y Tecnología (CONAHCyT) for the post-doctoral economic support for three authors (Aguilar-Ávila, Hinojosa-Ventura and Velázquez-Carriles).

Declarations

Conflict of interest Authors declare no conflict interest.

References

Aguilar-Urquizo E, Itza-Ortiz MF, Sangines-Garcia JR, Pineiro-Vázquez AT, Reyes-Ramirez A, Pinacho-Santana B (2020) Phytobiotic activity of *Piper auritum* and *Ocimum basilicum* on avian *E. coli*. Braz J Poult Sci https://doi.org/10.1590/1806-9061-2019-1167

Ahmadi F (2012) Impact of different levels of silver nanoparticles (Ag-NPs) on performance, oxidative enzymes and blood parameters in broiler chicks. Pak Vet J 26(3):325–328

Akar Z, Akay S, Ejder N, Düzgün AO (2023) Determination of the cytotoxicity and antibiofilm potential effect of *Equisetum arvense* silver nanoparticles. Appl Biochem Biotechnol. https://doi.org/10.1007/s12010-023-04587-7

Al-Rajhi AMH, Salem SS, Alharbi AA, Abdelghany TM (2022) Ecofriendly synthesis of silver nanoparticles using Kei-apple (*Dovyalis caffra*) fruit and their efficacy against cancer cells and clinical pathogenic microorganisms. Arab J Chem 15(7):03927. https://doi.org/10.1016/j.arabjc.2022.103927

Alharthi AF, Gouda M, Khalaf MM, Elmushyakhi A, Abou Taleb MF, Abd El-Lateef HM (2023) Cellulose-acetate-based films modified with Ag2O and ZnS as nanocomposites for highly controlling biological behavior for wound. Healing Appl Mater 16:777. https://doi.org/10.3390/ma16020777

Ali F, Younas U, Nazir A, Hassan F, Iqbal M, Hamza B, Mukhtar S, Khalid A, Ishfaq A (2022) Biosynthesis and characterization of silver nanoparticles using strawberry seed extract and evaluation of their antibacterial and antioxidant activities. J Saudi Chem Soc 26(6):101558. https://doi.org/10.1016/j.jscs.2022.101558

Amaliyah S, Sabarudin A, Masruri M, Sumitro SB (2022) Characterization and antibacterial application of

biosynthesized silver nanoparticles using *Piper retrofractum* vahl fruit extract as bioreductor. J Appl Pharm Sci 12(3):103–114. https://doi.org/10.7324/JAPS.2022.120311

Angulo A, Maldonado M, Delgado K, Reyes-Becerril M (2017) *Debaryomyces hansenii* up regulates superoxide dismutase gene expression and enhances the immune response and survival in pacific red snapper (*Lutjanus peru*) leukocytes after *Vibrio parahaemolyticus* infection. Dev Comp Immunol 71:18–27. https://doi.org/10.1016/j.dci.2017.01.020

Awad MA, Hendi AA, Ortashi KMO, Alanazi AB, ALZahrani BA, Soliman DA (2019) Greener synthesis, characterization, and antimicrobiological effects of *Helba* silver nanoparticle-PMMA nanocomposite. Int J Polym Sci 4379507:7. https://doi.org/10.1155/2019/4379507

Ayromlou A, Masoudi S, Mirzaie A (2019) *Scorzonera calyculata* aerial part extract mediated synthesis of silver nanoparticles: evaluation of their antibacterial, antioxidant and anticancer activities. J Clust Sci 30:1037–1050. https://doi.org/10.1007/s10876-019-01563-2

Banua J, Han JI (2020) Biogenesis of prism-like silver oxide nanoparticles using nappa cabbage extract and their p-nitrophenol sensing activity. Molecules 25(10):2298. https://doi.org/10.3390/molecules25102298

Benzie IF, Strain JJ (1996) The ferric reducing ability of plasma (FRAP) as a measure of antioxidant power: the FRAP assay. Anal Biochem 239(1):70–76. https://doi.org/10.1006/abio.1996.0292

Bhakya S, Muthukrishnan S, Sukumaran M, Muthukumar M (2022) Biogenic synthesis of silver nanoparticles and their antioxidant and antibacterial activity. Appl Nanosci 6:755–766. https://doi.org/10.1007/s13204-015-0473-z

Brand-Williams W, Cuvelier ME, Berset C (1995) Use of a free radical method to evaluate antioxidant activity. LWT-Food Sci Technol 28(1):25–30. https://doi.org/10.1016/S0023-6438(95)80008-5

Castorena-Sánchez A, Velázquez-Carriles CA, López-Álvarez MA, Serrano-Niño JC, Cavazos-Garduño A, Garay-Martínez LE, Silva-Jara JM (2023) Magnesium nanohydroxide (2D brucite) as a host matrix for thymol and carvacrol: synthesis, characterization, and inhibition of foodborne pathogens. Green Proc Synth 12(1):20230145. https://doi.org/10.1515/gps-2023-0145

Chacón C, Bojórquez-Quintal E, Caamal-Chan G, Ruíz-Valdiviezo VM, Montes-Molina JA, Garrido-Ramírez ER, Rojas-Abarca LM, Ruiz-Lau N (2021) In vitro antifungal activity and chemical composition of *Piper auritum* Kunth essential oil against *Fusarium oxysporum* and *Fusarium equiseti*. Agronomy 11(6):1098. https://doi.org/10.3390/agronomy11061098

Corciova A, Mircea C, Burlec AF, Cioanca O, Tuchilus C, Fifere A, Lungoci AL, Marangoci N, Hancianu M (2019) Antioxidant, antimicrobial and photocatalytic activities of silver nanoparticles obtained by bee propolis extract assisted biosynthesis. Farmacia 67(3):482–489. https://doi.org/10.31925/farmacia.2019.3.16

Dawadi S, Katuwal S, Gupta A, Lamichhane U, Thapa R, Jaisi S, Lamichhane G, Bhattarai DP, Parajuli N (2021) Current research on silver nanoparticles: synthesis, characterization, and applications. J Nanomater. https://doi.org/10.1155/2021/6687290

de Lacerda Coriolano D, Souza JB, Bueno Ev, Medeiros SMD-FRDS, Cavalcanti IDL, Cavalcanti IMF (2021) Antibacterial and antibiofilm potential of silver nanoparticles against antibiotic-sensitive and multidrug-resistant *Pseudomonas aeruginosa* strains. Braz J Microbiol 52:267–278. https://doi.org/10.1007/s42770-020-00406-x

Dewi FRP, Lim V, Rosyidah AA, Fatimah, Wahyuningsih SPA, Zubaidah U (2023) Characterization of silver nanoparticles (AgNPs) synthesized from *Piper ornatum* leaf extract and its activity against food borne pathogen *Staphylococcus aureus*. Biodivers J Biol Divers 24(3):1742–1748. https://doi.org/10.13057/biodiv/d240348

Dharmaraj D, Krishnamoorthy M, Rajendran K, Karuppiah K, Annamalai J, Durairaj KR, Santhiyagu P, Ethiraj K (2021) Antibacterial and cytotoxicity activities of biosynthesized silver oxide (Ag_2O) nanoparticles using *Bacillus paramycoides*. J Drug Deliv Sci Technol 61:102111. https://doi.org/10.1016/j.jddst.2020.102111

Dhoondia ZH, Chakraborty H (2012) *Lactobacillus* mediated synthesis of silver oxide nanoparticles. Nanomater Nanotechnol 2(15):1. https://doi.org/10.5772/55741

Essghaier B, Ben Khedher G, Hannachi H, Dridi R, Zid MF, Chaffei C (2022) Green synthesis of silver nanoparticles using mixed leaves aqueous extract of wild olive and pistachio: characterization, antioxidant, antimicrobial and effect on virulence factors of *Candida*. Arch Microbiol 204(4):203. https://doi.org/10.1007/s00203-022-02810-3

Fowsiya J, Madhumitha G (2019) Biomolecules derived from Carissa edulis for the microwave assisted synthesis of Ag2O nanoparticles: A study against *S. incertulas*, *C. medinalis* and *S. mauritia*. J Clust Sci 30(5):1243–1252. https://doi.org/10.1007/s10876-019-01627-3

Hetta HF, Al-Kadmy IMS, Khazaal SS, Abbas S, Suhail A, El-Mokhtar MA, Ellah NHA, Ahmed EA, Abd-ellatief RB, El-Masry EA, Batiha GES, Elkady AA, Mohamed NA, Algammal AM (2021) Antibiofilm and antivirulence potential of silver nanoparticles against multidrug-resistant *Acinetobacter baumannii*. Sci Rep 11:10751. https://doi.org/10.1038/s41598-021-90208-4

Ibrahim S, Ahmad Z, Manzoor MZ, Mujahid M, Faheem Z, Adnan A (2021) Optimization for biogenic microbial synthesis of silver nanoparticles through response surface methodology, characterization, their antimicrobial, antioxidant, and catalytic potential. Sci Rep 11(1):770. https://doi.org/10.1038/s41598-020-80805-0

Jabbar AH, Al-Janabi HSO, Hamzah MQ, Mezan SO, Tumah AN, Ameruddin ASB, Agam MA (2020) Green synthesis and characterization of silver nanoparticle (AgNPs) using *Pandanus atrocarpus* extract. Int J Adv Sci Technol 29(3):4913–4922

Jaswal T, Gupta J (2023) A review on the toxicity of silver nanoparticles on human health. Mater Today Proc 81(2):859–863. https://doi.org/10.1016/j.matpr.2021.04.266

Kanniah P, Chelliah P, Thangapandi JR, Gnanadhas G, Mahendran V, Robert M (2021) Green synthesis of antibacterial and cytotoxic silver nanoparticles by *Piper nigrum* seed extract and development of antibacterial silver based Chitosan Nanocomposite. Int J Biol Macromol 189:18–33. https://doi.org/10.1016/j.ijbiomac.2021.08.056

Kemenade B, Groeneveld A, Rens B, Rombout J (1994) Characterization of macrophages and neutrophilic granulocytes from the pronephros of carp (*Cyprinus carpio* L). J Exp Biol 187(1):143–158. https://doi.org/10.1242/jeb.187.1.143

Li H, Wang X, Li P, Li Y, Wang H (2008) Comparative study of antioxidant activity of grape (*Vitis vinifera*) seed powder assessed by different methods. J Food Drug Anal 16(6):67–73. https://doi.org/10.38212/2224-6614.2321

Liu X, Yao H, Zhao X, Ge C (2023) Biofilm formation and control of foodborne pathogenic bacteria. Molecules 28(6):2432. https://doi.org/10.3390/molecules28062432

Manik UP, Nande A, Raut S, Dhoble SJ (2020) Green synthesis of silver nanoparticles using plant leaf extraction of *Artocarpus heterophylus* and *Azadirachta indica*. Results Mater 6:100086. https://doi.org/10.1016/j.rinma.2020.100086

Manikandan V, Velmurugan P, Park JH, Chang WS, Park YJ, Jayanthi P, Cho M, Oh BT (2017) Green synthesis of silver oxide nanoparticles and its antibacterial activity against dental pathogens. 3 Biotech 7:1–9. https://doi.org/10.1007/s13205-017-0670-4

Morillo-Castillo JA, Balseca-Ibarra MC (2018) Inhibitory effect of the essential oil of Cymbopogon citratus on the strain of *Porphyromona gingivalis*: in vitro study. Odontología 20(2):5–13. https://doi.org/10.29166/odontologia.vol20.n2.2018-5-13

Nguyen VP, Trung HL, Nguyen TH, Hoang D, Tran TH (2021) Synthesis of biogenic silver nanoparticles with eco-friendly processes using *Ganoderma lucidum* extract and evaluation of their theranostic applications. J Nanomater Article ID 6135920:11. https://doi.org/10.1155/2021/6135920

O'Toole GA (2011) Microtiter dish biofilm formation assay. J Vis Exp 47:2437. https://doi.org/10.3791/2437

Ognik K, Cholewińska E, Czech A, Kozlowski K, Wlazlo L, Nowakowicz-Dębek B, Szlązak R, Tutaj K (2016) Effect of silver nanoparticles on the immune, redox, and lipid status of chicken blood. Czech J Anim Sci 61(10):450–461. https://doi.org/10.17221/80/2015-CJAS

Paunovic J, Vucevic D, Radosavljevic T, Mandić-Rajčević S, Pantic I (2020) Iron-based nanoparticles and their potential toxicity: focus on oxidative stress and apoptosis. Chem Biol Interac 316:108935. https://doi.org/10.1016/j.cbi.2019.108935

Perez Gutierrez RM (2016) Antidiabetic andantioxidant properties, and α-amylase and α-glucosidase inhibition effects of triterpene saponins from *Piper auritum*. Food Sci Biotechnol 25(1):229–239. https://doi.org/10.1007/s10068-016-0034-6

Riss TL, Moravec RA, Niles AL, Duellman S, Benink HA, Worzella TJ, Minor L (2016) Cell viability assays. Assay guidance manual. Eli Lilly & Company and the National Center for Advancing Translational Sciences, Bethesda, pp 1–23

Romero-García DM, Velázquez-Carriles CA, Gomez C, Velázquez-Juárez G, Silva-Jara JM (2023) Tannic acid-layered hydroxide salt hybrid: assessment of antibiofilm formation and foodborne pathogen growth inhibition. J Food Sci Technol 60(10):2659–2669. https://doi.org/10.1007/s13197-023-05790-4

Salleh WMNHW (2021) A systematic review of botany, phytochemicals and pharmacological properties of *Hoja Santa* (*Piper auritum* Kunth). Z Naturforsch C J Biosci 76(3–4):93–102. https://doi.org/10.1515/znc-2020-0116

Shehabeldine AM, Elbahnasawy MA, Hasaballah AI (2021) Green phytosynthesis of silver nanoparticles using *Echinochloa stagnina* extract with reference to their antibacterial, cytotoxic, and larvicidal activities. BioNanoScience 11:526–538. https://doi.org/10.1007/s12668-021-00846-1

Silva-Jara J, Angulo C, Macías ME, Velazquez C, Guluarte C, Reyes-Becerril M (2020) First screening report of immune and protective effect of non-toxic *Jatropha vernicosa* stem bark against *Vibrio parahaemolyticus* in Longfin Yellowtail *Seriola rivoliana* leukocytes. Fish Shellfish Immunol 101:106–114. https://doi.org/10.1016/j.fsi.2020.03.048

Singleton VL, Orthofer R, Lamuela-Raventós RM (1999) Analysis of total phenols and other oxidation substrates and antioxidants by means of folin-ciocalteu reagent. Meth Enzymol 299:152–178. https://doi.org/10.1016/S0076-6879(99)99017-1

Sneha T, Krishna MG, Sandhya RM (2017) Plant-mediated synthesis of silver nanoparticles—a critical review. Int J Pharmacogn Phytochem 9(7):947–956. https://doi.org/10.25258/phyto.v9i07.11161

Tang KWK, Millar BC, Moore JE (2023) Antimicrobial resistance (AMR). Br J Biomed Sci 80:11387. https://doi.org/10.3389/bjbs.2023.11387

Wang M, Zhu P, Zhao S, Nie C, Wang N, Du X, Zhou Y (2017) Characterization, antioxidant activity and immunomodulatory activity of polysaccharides from the swollen culms of *Zizania latifolia*. Int J Biol Macromol 95:809–817. https://doi.org/10.1016/j.ijbiomac.2016.12.010